BRAIN
A JOURNAL OF NEUROLOGY

Dissecting phenotypic traits linked to human resilience to Alzheimer's pathology

Beatriz G. Perez-Nievas,[1] Thor D. Stein,[1] Hwan-Ching Tai,[1] Oriol Dols-Icardo,[1] Thomas C. Scotton,[1] Isabel Barroeta-Espar,[1] Leticia Fernandez-Carballo,[1] Estibaliz Lopez de Munain,[1] Jesus Perez,[1] Marta Marquie,[1] Alberto Serrano-Pozo,[1] Mathew P. Frosch,[1] Val Lowe,[2] Joseph E. Parisi,[3] Ronald C. Petersen,[4] Milos D. Ikonomovic,[5,6] Oscar L. López,[5] William Klunk,[7] Bradley T. Hyman[1] and Teresa Gómez-Isla[1]

1 Massachusetts General Hospital ADRC, Harvard University, Boston, MA, USA
2 Department of Diagnostic Radiology, Mayo Clinic and Foundation, Rochester, MN, USA
3 Laboratory Medicine and Pathology, Mayo Clinic, Rochester, MN, USA
4 Department of Neurology, Mayo Clinic, Rochester, MN, USA
5 Department of Neurology, University of Pittsburgh School of Medicine, Pittsburgh, USA
6 Geriatric Research Education and Clinical Center, VA Pittsburgh Healthcare System Pittsburgh, Pennsylvania, United States
7 Departments of Psychiatry and Neurology, University of Pittsburgh School of Medicine, Pittsburgh, PA, USA

Correspondence to: Teresa Gómez-Isla, MD, PhD,
Neurology Department,
Massachusetts General Hospital,
15th Parkman St, Boston MA 02114,
USA
E-mail: tgomezisla@partners.org

Clinico-pathological correlation studies and positron emission tomography amyloid imaging studies have shown that some individuals can tolerate substantial amounts of Alzheimer's pathology in their brains without experiencing dementia. Few details are known about the neuropathological phenotype of these unique cases that might prove relevant to understanding human resilience to Alzheimer's pathology. We conducted detailed quantitative histopathological and biochemical assessments on brains from non-demented individuals before death whose brains were free of substantial Alzheimer's pathology, non-demented individuals before death but whose post-mortem examination demonstrated significant amounts of Alzheimer's changes ('mismatches'), and demented Alzheimer's cases. Quantification of amyloid-β plaque burden, stereologically-based counts of neurofibrillary tangles, neurons and reactive glia, and morphological analyses of axons were performed in the multimodal association cortex lining the superior temporal sulcus. Levels of synaptic integrity markers, and soluble monomeric and multimeric amyloid-β and tau species were measured. Our results indicate that some individuals can accumulate equivalent loads of amyloid-β plaques and tangles to those found in demented Alzheimer's cases without experiencing dementia. Analyses revealed four main phenotypic differences among these two groups: (i) mismatches had striking preservation of neuron numbers, synaptic markers and axonal geometry compared to demented cases; (ii) demented cases had significantly higher burdens of fibrillar thioflavin-S-positive plaques and of oligomeric amyloid-β deposits reactive to conformer-specific antibody NAB61 than mismatches; (iii) strong and selective accumulation of hyperphosphorylated soluble tau multimers into the synaptic compartment was noted in demented cases compared with controls but not in mismatches; and (iv) the robust glial activation accompanying amyloid-β and tau pathologies in demented cases was remarkably reduced in mismatches. Further biochemical measurements of soluble amyloid-β species—monomers, dimers and higher molecular weight oligomers—in total brain homogenates and synaptoneurosomal preparations failed to demonstrate significant differences between mismatches and demented cases. Together, these data suggest that amyloid-β plaques and tangles do not inevitably result in neural system derangement and dementia in all

individuals. We identified distinct phenotypic characteristics in the profile of brain fibrillar and soluble amyloid-β and tau accrual and in the glial response that discriminated demented and non-demented individuals with high loads of Alzheimer's pathology. Amyloid-β deposition in the form of fibrillar plaques and intimately related oligomeric amyloid-β assemblies, hyperphosphorylated soluble tau species localized in synapses, and glial activation emerged in this series as likely mediators of neurotoxicity and altered cognition, providing further insight into factors and pathways potentially involved in human susceptibility or resilience to Alzheimer's pathological changes.

Introduction

Increasing evidence suggests that there can be dissociation between occurrence of Alzheimer's disease pathology and clinical symptoms of dementia. In the Nun Study, where individuals volunteered for autopsy regardless of symptoms, 12% of participants with intact cognition at time of death had abundant amyloid-β plaques and neurofibrillary tangles, the two chief pathological hallmarks of Alzheimer's disease, at post-mortem examination (Riley et al., 2005). Consistent with these observations, data from the Religious Orders Study and the Memory and Aging Project showed that one-third of brains from older people without cognitive impairment demonstrated enough Alzheimer's disease lesions to meet pathological criteria for Alzheimer's disease (Schneider et al., 2009). Amyloid neuroimaging has made it possible to identify amyloid deposition in vivo (Klunk et al., 2004) and recent studies have suggested that Pittsburgh compound B binds to fibrillar amyloid-β deposits (Lockhart et al., 2007; Ikonomovic et al., 2008). Elevated Pittsburgh compound B retention has been reported in >20% of clinically unimpaired elderly volunteers (Lopresti et al., 2005; Mintun et al., 2006; Rowe et al., 2007; Aizenstein et al., 2008). Altogether, the above data suggest that some individuals can remain asymptomatic for dementia while alive despite having substantial amounts of Alzheimer's disease pathology in their brains.

Little is known about these unique cases that may prove valuable to identify factors and pathways responsible for human resilience to Alzheimer's disease and help guide the design of novel neuroprotective therapies. In fact, fundamental questions remain unanswered. Why do they not get demented? Are their neurons and synapses truly preserved? Is the form of amyloid-β or tau (the two main components of plaques and tangles, respectively) accumulated in the brain e.g. soluble amyloid-β/tau species versus fibrillar plaques/tangles; what determines structural damage and impaired cognition in Alzheimer's disease?

It has been recently proposed that soluble amyloid-β, and specifically soluble oligomeric forms of amyloid-β, rather than plaques themselves, could play a larger role in synaptic and neuronal damage and cognitive impairment in Alzheimer's disease (Selkoe, 1991; Shankar et al., 2008; Mc Donald et al., 2010). Favouring this possibility, recent data in humans suggested that soluble amyloid-β oligomers strongly correlate with cognitive impairment in Alzheimer's disease (Tomic et al., 2009; Mc Donald et al., 2010). Alternatively, or in addition to soluble amyloid-β, forms of soluble tau could also play a substantial role in neural system disruption and altered cognition in Alzheimer's disease. Supporting

this notion, two recent studies identified potentially neurotoxic soluble tau species that correlated with memory loss and neuronal cell loss in the absence of tangles in the brain of mouse tauopathy models and patients with Alzheimer's disease and frontotemporal dementia and parkinsonism linked to chromosome 17 (FTDP-17) (Berger et al., 2007; Hampton et al., 2010).

The present study was designed to test the idea that amyloid-β plaques and tangles do not inevitably result in neural system derangement and dementia in all individuals, and that a differential profile in brain accrual of potentially neurotoxic soluble amyloid-β and/or tau species may explain human resilience to Alzheimer's disease pathology. To confirm or refute these hypotheses, we conducted detailed quantitative neuropathological and biochemical assessments on post-mortem brain samples containing the banks of the superior temporal sulcus from (i) non-demented individuals before death whose post-mortem examination demonstrated absence of substantial Alzheimer's disease pathology; (ii) non-demented individuals before death but whose post-mortem examination demonstrated abundant Alzheimer's disease pathology (we refer to them as 'mismatches'); and (iii) individuals with Alzheimer's disease pathology and dementia. Our results suggest that some individuals may accumulate equivalent burdens of amyloid-β plaques and neurofibrillary tangles in high order association cortex to those found in demented cases with Alzheimer's disease without experiencing dementia or suffering substantial structural damage in their neuronal populations. Indeed, mismatches had striking preservation of neuronal and synaptic elements and axonal geometry despite high levels of Alzheimer's disease pathology. We did not find significant differences between mismatches and demented cases when we measured soluble species of amyloid-β (monomers, dimers and higher molecular weight oligomers) in whole brain homogenates or synaptoneurosomal preparations using western blot and ELISA assays. However, we observed significantly higher loads of fibrillar thioflavin S-reactive plaques and oligomeric amyloid-β deposits recognized by conformer-specific antibody NAB61, and aberrant accumulation of hyperphosphorylated soluble tau in synapses in demented cases. These differential phenotypic traits in demented cases were accompanied by a robust glial response, with a significant increase in the number of reactive astrocytes and microglial cells that was markedly reduced in mismatches. Altogether, our results suggest that the load of classical fibrillar thioflavin-S-reactive plaques in the brain, but not the amount of total amyloid-β plaques (fibrillar plus non-fibrillar) or tangles, and some of the changes preferentially associated with that subset of plaques (e.g. oligomeric amyloid-β deposits, aberrant accumulation of soluble phospho-tau into the

synaptic compartment, and glial reaction) predict anatomical neural system disruption and dementia, and differentiate classical demented cases with Alzheimer's disease from individuals who seem to tolerate high loads of Alzheimer's disease pathology in their brains.

Material and methods

Human brain samples

The study included 50 cases combined from Massachusetts General Hospital, Mayo Clinic and University of Pittsburgh ADRC Brain Banks. Cases were scored by the Consortium to Establish a Registry for Alzheimer's Disease (CERAD) scale for neuritic plaques (A–C) and Braak stage for neurofibrillary tangles (0–VI). According to the National Institute on Aging and Reagan Institute, there is a high probability of a diagnosis of Alzheimer's disease if there are frequent neuritic plaques and high Braak stage of neurofibrillary tangles (CERAD C, Braak V/VI), an intermediate probability if there is a moderate density of neuritic plaques and neurofibrillary tangles in a limbic distribution (CERAD B, Braak III/IV), and a low probability if there is a scarce distribution of neuritic plaques and neurofibrillary tangles (CERAD A and Braak I/II) (The NIA-RIA Working group, 1997). Cases were divided in four groups according to these criteria: (i) non-demented individuals before death whose post-mortem exam demonstrated low probability of Alzheimer's disease, termed 'controls' ($n = 15$); (ii) non-demented individuals before death but whose post-mortem examination demonstrated intermediate probability of Alzheimer's disease, termed 'intermediate probability mismatches' ($n = 12$); (iii) non-demented individuals before death but whose post-mortem examination demonstrated high probability of Alzheimer's disease, termed 'high probability mismatches' ($n = 8$); and (iv) demented individuals before death whose post-mortem examination demonstrated high probability of Alzheimer's disease, termed 'cases with Alzheimer's disease' ($n = 15$). One-third of non-demented cases, including three of eight high probability mismatches, had been clinically seen with formal cognitive evaluation within 2 years of death. The rest were individuals with no reported dementia according to their clinical records and death certificates. Histological evaluation was performed on a set of blocked regions representative for a spectrum of neurodegenerative diseases; all blocks were stained with Luxol fast blue and haematoxylin and eosin, and selected blocks were stained for Bielschowsky silver stain and amyloid-β, alpha-synuclein, ubiquitin and phospho-tau immunoreactivity. Neuropathological diagnosis was recorded, and cases with evidence of brain infarcts, cortical Lewy bodies or other lesions different to Alzheimer's disease pathology were excluded.

Quantitative neuropathology

Quantitative neuropathological assessments were performed in multimodal association cortex lining the upper and lower bank of the superior temporal sulcus that consistently undergoes amyloid-β deposition, neurofibrillary tangle formation and neuronal loss in Alzheimer's disease (Gomez-Isla *et al.*, 1997). Morphological phenotypes were derived by immunostaining 50-μm thick formalin fixed sections with 10D5 antibody to label amyloid-β plaques (1:50, Elan Pharmaceuticals), NAB61 antibody to label oligomeric amyloid-β deposits (1:100, kind gift of Dr. Virginia Lee, University of Pennsylvania) (Lee *et al.*, 2006), PHF-1 antibody to label neurofibrillary tangles (1:100, kind gift of Dr. Peter Davies), NeuN antibody to label neurons (1:200; Chemicon), GFAP antibody to label activated astrocytes (1:500, Chemicon) and CD68 antibody to label activated microglia (1:100, Dako), followed by the appropriate secondary antibody (horseradish peroxidase anti-mouse or anti-rabbit IgG 1:200, Southern Biotechnology; Vector ABC Kit). Sections were also stained with thioflavin-S for fibrillar amyloid-β plaques and analysed using a microscope equipped with a digital camera, linked to a computerized image analysis system running Bioquant software (R and M Biometrix). Amyloid-β plaque deposition was quantified according to protocols previously published (Gomez-Isla *et al.*, 1997; Irizarry *et al.*, 1997). Total amyloid-β plaque burden, defined as total percentage of superior temporal sulcus per section covered by 10D5 immunostained deposits; fibrillar amyloid-β plaque burden defined as total percentage of superior temporal sulcus per section covered by thioflavin-S positive amyloid-β plaques; and average plaque size were calculated in each case. Stereologically-based counts of neurofibrillary tangles, neurons, GFAP-positive astrocytes and CD68-positive microglial cells were performed as previously described (West and Gundersen, 1990; Gomez-Isla *et al.*, 1996). Superior temporal sulcus cortical thickness was measured on Nissl stained sections as additional measure of anatomical integrity.

Axonal trajectory and morphology analyses

To visualize axons, tissue was incubated with SMI-312 antibody (1:1000, Covance Research Products) and a secondary anti-mouse antibody conjugated with cyanine 3 (1:200, Jackson Immuno-Research), and then counterstained with thioflavin-S (0.05% in 50% ethanol). Analysis of axonal ratio curvature was conducted using ImageJ software from the NIH and according to previously published protocols (Spires-Jones *et al.*, 2009). Axon segments longer than 20 μm were analysed and their curvature ratio was calculated by dividing the curvilinear length of the axon segment by the straight line length of the process. Axons closer than 50 μm to a plaque were defined as 'close to plaques' and others as 'far from plaques'. Number of neuritic dystrophies per plaque (size of dystrophies defined as areas of neurite swelling >2.5 μm in diameter) was also assessed.

Measures of synaptic markers and soluble amyloid-β and tau species in total brain homogenates and synaptoneurosomes

Levels of postsynaptic density protein 95 (PSD-95), a postsynaptic marker, and synaptophysin, a presynaptic marker, were measured in total homogenates from frozen samples containing the superior temporal sulcus by SDS-PAGE immunoblotting technique using the appropriate primary (PSD-95 1:1000 Cell Signaling; Synaptophysin

1:1000 Millipore) and secondary antibodies (horseradish peroxidase anti-mouse or anti-rabbit IgG 1:2000, Bio-Rad). Amyloid-β monomers and oligomers were detected in frozen samples containing the superior temporal sulcus sequentially extracted with Tris-buffered saline (TBS), 1% Triton™ X-100 and 2% SDS. Total homogenates were centrifuged at 260 000g for 30 min at 4°C, and the supernatant was collected as the Tris-buffered saline soluble fraction. The pellet was detached and an equivalent volume of 1% Triton™ X-100 was added. Then the pellet was homogenized and centrifuged at 260 000g for 30 min at 4°C, and the supernatant was collected as the Triton-X soluble fraction. This second pellet was detached and an equivalent volume of 2% SDS was added. The pellet was again homogenized, the tubes were kept at 37°C for 30 min, then centrifuged at 260 000g for 30 min at room temperature, and the supernatant was collected as the SDS soluble fraction. Three different methods were used to detect and quantify soluble amyloid-β species: (i) SDS-PAGE immunoblotting with a mixture of two amyloid-β N-terminal monoclonal antibodies, 82E1 (IBL) and 6E10 (Covance), to increase detection sensitivity (Hashimoto *et al.*, 2012); (ii) two-site sandwich ELISA kit (Wako) that uses the well-characterized BNT77/BA27 antibody pair to detect amyloid-β_{40}, following the manufacturer's protocol. Briefly, samples were loaded in duplicates onto microplates precoated with antibody specific to amyloid-β_{11-28}, BNT77 and detected with horseradish peroxidase-conjugated BA27 antibody, which specifically detects the C terminus of amyloid-β_{40}. The absorbance of each well at 450 nm was determined with a 96-plate reader (Wallac 1420 VICTOR2, Perkin Elmer); and (iii) human amyloid-β oligomers (82E1-specific) assay kit (IBL International), based on a same site sandwich phase ELISA specific for dimers and higher molecular weight amyloid-β oligomers, following the manufacturer's protocol. In brief, samples were loaded in quadruplicates onto microplates precoated with 82E1 and detected with horseradish peroxidase-conjugated 82E1, a mouse monoclonal antibody that recognizes the N-terminus of human amyloid-β specifically, with two or more epitopes. The absorbance of each well at 450 nm was determined with a 96-plate reader (Wallac 1420 VICTOR2, Perkin Elmer). Amyloid-β monomers and dimers were also detected and measured in synaptoneurosomes prepared according to previously published protocols as briefly described below (Tai *et al.*, 2012), by SDS-PAGE immunoblotting and 82E1 plus 6E10 antibodies.

Levels of soluble tau were assessed in cytosolic and synaptic fractions from frozen samples containing the superior temporal sulcus using western blot and specific antibodies against human tau (H7, Dako) and phospho-tau (PHF-1, kind gift of Dr. Peter Davies). Synaptoneurosomes were prepared from ~250 mg of frozen tissue (grey matter). Tissue was homogenized in 1.5 ml cold Buffer A (25 mM HEPES, pH 7.9, 120 mM NaCl, 5 mM KCl, 1 mM MgCl$_2$, 2 mM CaCl$_2$, 1 mM dithiothreitol, protease inhibitors, phosphatase inhibitors) using a Teflon-glass mechanical tissue grinder at 170 rpm and filtered through 80 μm pore filters. A small portion of the filtrate was supplemented with 1.5% SDS, boiled for 5 min, and centrifuged at 15 000g for 15 min, and the supernatant was collected as total extract. The other portion was further filtered through 5 μm pore filters and centrifuged at 1000g for 10 min to pellet synaptoneurosomes. The supernatant was

collected as cytosolic extract, which was further centrifuged at 100 000g for 30 min to remove microsomes. The synaptoneurosome pellet was washed once with cold Buffer A and centrifuged again at 1000g for 10 min. The pellet was extracted with 0.5 ml Buffer B (50 mM Tris pH 7.5, 1.5% SDS, 2 mM dithiothreitol) and boiled for 5 min. After centrifugation at 15 000g for 15 min, the supernatant was collected as synaptoneurosomal extract. Synaptophysin and PSD-95 were used for purity control of the extracts.

Statistical analyses

Kolmogorov-Smirnov test was used for analysis of normality. For variables with normal distribution one-way ANOVA followed by Tukey *post hoc* comparison was used to detect differences among groups. Non-parametric Kruskal-Wallis one-way ANOVA and Dunn's multiple comparison test were used to detect differences among groups for variables with non-normal distributions. In all tests the level of significance was at $P < 0.05$. Data are presented as mean ± standard error, unless otherwise indicated.

Results

Table 1 summarizes the descriptive statistics for demographics and quantitative neuropathological assessments. Average age at death mismatches with high and intermediate probability was about a decade older than the overall average life expectancy in the USA, 78.1 years in 2008 according to the National Center for Health Statistics (Arias, 2012), indicating that mismatches were generally long-lived individuals. Controls and demented cases with Alzheimer's disease were selected to match the ages of mismatches.

Total amyloid-β plaque burden and number of neurofibrillary tangles in the superior temporal sulcus region did not distinguish high probability mismatches from demented Alzheimer's disease cases

The percentage of superior temporal sulcus covered by 10D5-positive amyloid-β deposits (total amyloid-β plaque burden), including diffuse and fibrillar amyloid-β plaques, was significantly higher in demented cases with Alzheimer's disease compared with intermediate probability mismatches and controls (Table 1, Fig. 1A and B) but did not significantly differ from high probability mismatches. Number of neurofibrillary tangles in the superior temporal sulcus was also significantly higher in demented cases with Alzheimer's disease than in intermediate probability mismatches but did not significantly differ from that found in high probability mismatches (Table 1, Fig. 1C and D). Controls were essentially free of neurofibrillary tangles in this area. These data indicate that some individuals (high probability mismatches) may remain free of dementia despite having accumulated amounts of

Table 1 Descriptive statistics for demographics and quantitative neuropathological assessments

|	Control (n = 15)	Intermediate probability mismatches (n = 12)	High probability mismatches (n = 8)	Alzheimer's disease (n = 15)
Age (years)	84.44 ± 3.20	89.82 ± 2.72	88.4 ± 6.01	87.2 ± 3.22
10D5 Amyloid-β plaque burden (%)	1.25 ± 0.56	3.58 ± 0.88	6.49 ± 1.55*	10.7 ± 1.13***
Thioflavin-S plaque burden (%)	0.28 ± 0.15	1.14 ± 0.45	0.55 ± 0.22	2.75 ± 0.7**
NAB61 oligomeric burden (%)	0.31 ± 0.14	1.34 ± 0.54	0.66 ± 0.41	4.79 ± 0.72***
NFTs/50-μm thick section	7 ± 3	40 ± 12	5509 ± 1536***	6670 ± 1122***
Neurons/50-μm thick section	171 070 ± 9457	159 808 ± 12 255	160 858 ± 5055**	104 721 ± 2322***
Cortical thickness (μm)	3035 ± 116	2955 ± 83	3154 ± 188	2421 ± 99**
GFAP-positive astrocytes/50-μm thick section	7243 ± 1811	6497 ± 1,117	5759 ± 1,157	14 728 ± 1959*
CD68-positive microglia/50-μm thick section	1435 ± 688.1	2994 ± 1,441	2208 ± 1066	15 748 ± 2580**

*$P < 0.05$; **$P < 0.01$; ***$P < 0.001$ versus control.
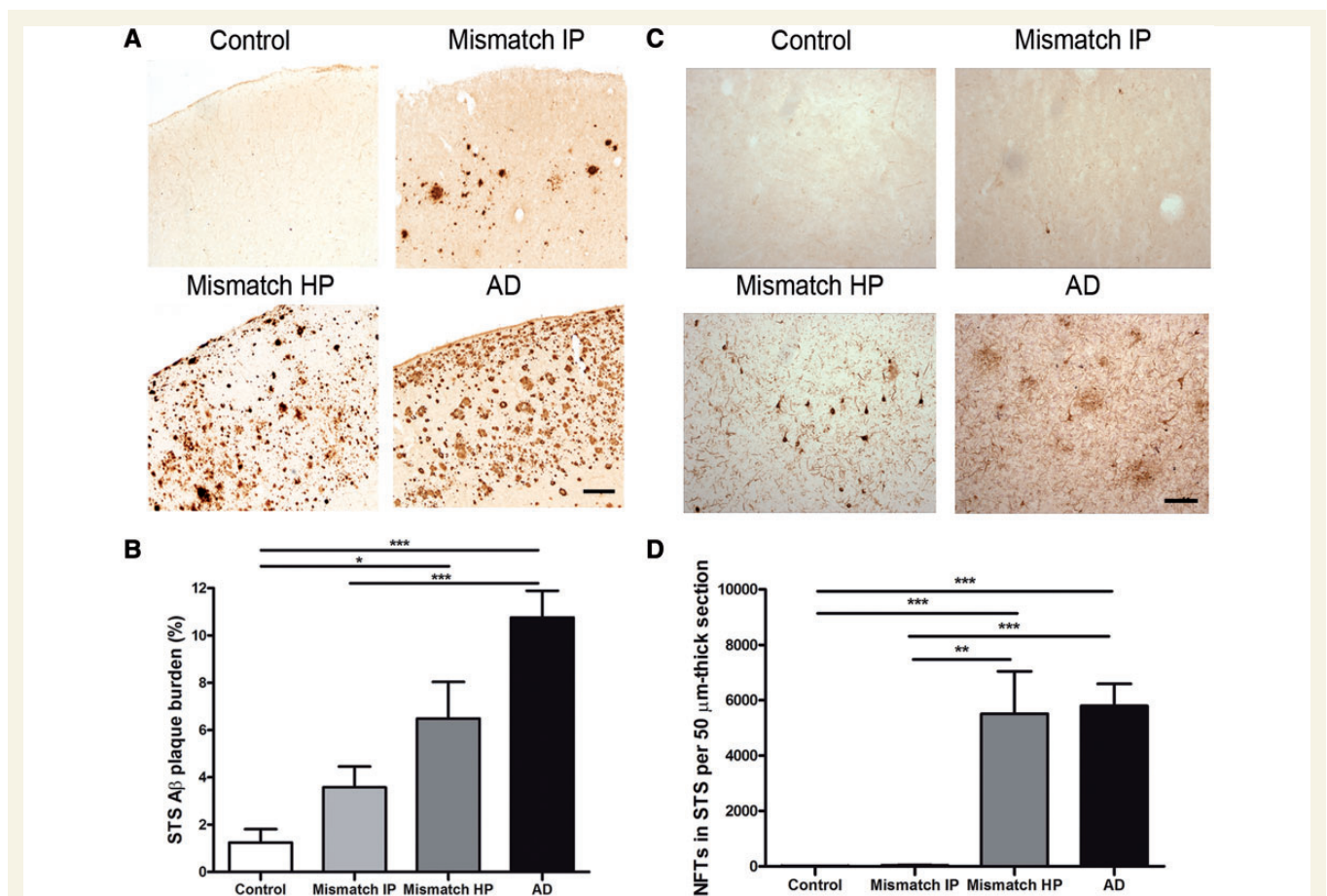
Figure 1 Amyloid-β plaque burden and number of neurofibrillary tangles in the superior temporal sulcus (STS). (**A**) Representative photomicrographs of 10D5 immunostained plaques in the superior temporal sulcus. (**B**) Demented cases with Alzheimer's disease (AD) had a significantly higher amyloid-β plaque burden in the superior temporal sulcus when compared with intermediate probability mismatches (Mismatch IP) and controls. No significant differences were found between demented cases with Alzheimer's disease and high probability mismatches (Mismatch HP). (**C**) Representative photomicrographs of PHF-1 immunostained neurofibrillary tangles in the superior temporal sulcus. (**D**) A significantly higher number of neurofibrillary tangles (NFTs) in the superior temporal sulcus were found in demented cases with Alzheimer's disease when compared with intermediate probability mismatches. No significant differences were detected in the number of neurofibrillary tangles between cases with Alzheimer's disease and high probability mismatches. Controls were essentially free of neurofibrillary tangles in this brain area. Scale bar = 150 μm; $n = 8$–15 per group; *$P < 0.05$; **$P < 0.01$; ***$P < 0.001$. One way ANOVA and *post hoc* Tukey test, and Kruskal-Wallis ANOVA and Dunn's multiple comparison test, respectively.

amyloid-β plaques and neurofibrillary tangles in their brains comparable to those seen in demented cases with Alzheimer's disease.

Number of neurons, cortical thickness and markers of synaptic integrity in the superior temporal sulcus were preserved in high probability mismatches but not in demented Alzheimer's disease cases

In Alzheimer's disease brains there is massive neuronal cell death, especially in limbic and association cortices that leads to brain gross atrophy, and loss of pre and postsynaptic structures that likely contribute to neural system dysfunction and cognitive deficits (reviewed in Gomez-Isla et al., 2008). We performed stereological neuronal counts and measured the cortical thickness in the superior temporal sulcus area in this series. In agreement with previous observations (Gomez-Isla et al., 1996) we noted a significant reduction of about 40% in the number of superior temporal sulcus neurons, and of about 20% in the cortical thickness in demented cases with Alzheimer's disease compared with controls whereas no significant neuronal loss or decrease in cortical thickness could be demonstrated in intermediate or high probability mismatches (Fig. 2A and B). Consistent with these results, levels of PSD-95, a prominent scaffolding neuronal component of the postsynaptic density, were significantly decreased by ~50% in demented cases with Alzheimer's disease but unchanged in high probability mismatches in comparison to controls (Fig. 2C). Levels of synaptophysin, an integral membrane glycoprotein ubiquitously present in presynaptic vesicles, were also significantly lower by about 50% in demented cases with Alzheimer's disease compared to controls, but not in high probability mismatches (Fig. 2D). A trend towards a higher level of PSD-95 and significantly higher levels of synaptophysin were noted in intermediate probability mismatches compared with controls; we believe this may represent an early synaptic compensatory mechanism in individuals with moderate amounts of Alzheimer's disease pathology and no dementia.

The above data confirm previous studies showing substantial loss of neurons in high order association cortex and of synaptic integrity markers in demented cases with Alzheimer's disease (Dekosky and Scheff, 1990; Gomez-Isla et al., 1996, 1997; Giannakopoulos et al., 2003; Scheff and Price, 2003). But they also demonstrate that in some unique human brains these selectively vulnerable neuronal populations, and their synaptic markers, are preserved despite robust amyloid-β deposition and neurofibrillary tangle formation.

Axonal morphology was better preserved in high probability mismatches than in demented Alzheimer's disease cases

Studies in humans and transgenic mice have demonstrated a widespread alteration in the geometry and morphology of dendrites and axons, including disrupted trajectories and dystrophic swellings, which occurs both near plaques, especially fibrillar thioflavin-S reactive plaques, but also distant from them in Alzheimer's disease (Knowles et al., 1999; Le et al., 2001; D'Amore et al., 2003; Spires et al., 2005; Coma et al., 2010; DaRocha-Souto et al., 2012). These changes likely contribute to altered neural system function and cognitive impairment in Alzheimer's disease. We analysed curvature ratio of axons in the superior temporal sulcus and observed that demented cases with Alzheimer's disease had significantly curvier axons than high probability mismatches and controls (Fig. 3A and B). When distance from a thioflavin-S-positive plaque was taken into account, axons were significantly curvier close to plaques ($<50\,\mu m$) than far from them ($>50\,\mu m$) both in demented cases with Alzheimer's disease and high probability mismatches (Fig. 3A and B). However, in high probability mismatches axons close to plaques were significantly less distorted than in demented cases with Alzheimer's disease (Fig. 3A and B), and axons far from plaques had normal straight trajectories indistinguishable from control cases, whereas in demented cases with Alzheimer's disease axons far from plaques were also significantly curvier than in controls (Fig. 3B). Moreover, a significantly higher number of neuritic dystrophies were seen in association with thioflavin-S-positive plaques in demented cases with Alzheimer's disease in comparison with high probability mismatches (Fig. 3C). These results demonstrate that the morphology and geometry of axons is much better preserved in high probability mismatches than in demented cases with Alzheimer's disease, despite similar total amyloid-β plaque burdens, and this may explain in part the absence of dementia in the former group.

Thioflavin-S-positive fibrillar plaque load in the superior temporal sulcus region was significantly higher in demented cases with Alzheimer's disease than in high probability mismatches

We investigated whether the amyloid-β phenotype (specific amyloid-β plaque subpopulations and/or soluble amyloid-β species) might impact the differences between mismatches and demented cases. We focused on the so-called 'neuritic' plaques that in general contain a core of amyloid histologically positive for dyes that stain β-pleated sheets and are often surrounded focal areas of neuronal loss and glial activation, dystrophic neurites and oligomeric amyloid-β deposits in Alzheimer's disease brains. Our previous data suggested that this subpopulation of plaques correlates much better than total amount of amyloid-β plaques with neuronal loss and impaired cognition in patients with Alzheimer's disease and transgenic mice (Gomez-Isla et al., 1997; DaRocha-Souto et al., 2011). In agreement with those observations, the superior temporal sulcus fibrillar thioflavin-S-positive plaque burden, but not the total amyloid-β plaque burden, was significantly higher in demented cases with Alzheimer's disease when compared with high probability mismatches (Table 1 and Fig. 4). Interestingly, although the number of fibrillar thioflavin-S-positive plaques did not significantly differ between the two groups (data

not shown), the average plaque size was significantly larger in demented cases with Alzheimer's disease than in high probability mismatches (1133 ± 153 μm^2 versus 131 ± 4.5 μm^2, respectively) (P < 0.001) accounting for the larger percentage of cortex covered by fibrillar thioflavin-S-positive plaques found in the former group as it is illustrated in Fig. 4.

Levels of soluble amyloid-β species measured by immunoblotting and ELISA did not differ among groups with a high burden of Alzheimer's disease pathology, but NAB61 reactive oligomeric amyloid-βload was higher in demented cases with Alzheimer's disease

It has been proposed that soluble oligomeric amyloid-β species could be a toxic moiety that plays a larger role in synapse and neuronal damage and cognitive impairment than plaques themselves (Selkoe, 1991; Shankar *et al*., 2008; Mc Donald *et al*., 2010). If this is correct, soluble amyloid-β levels should predict impaired cognition and disruption of brain anatomy. We measured levels of amyloid-β monomers and dimers in whole brain homogenates containing the superior temporal sulcus using sequential extractions yielding fractions that are hypothesized to be enriched with soluble proteins from distinct anatomical compartments: Tris-buffered saline (extracellular soluble), 1% Triton^{TM} X-100 (intracellular soluble) and 2% SDS (membrane-associated) using specific antibodies against amyloid-β and western blot (Fig. 5A–E). As shown in Fig. 5B and C, the levels of monomeric amyloid-β, corresponding to the band detected at 4 kDa, in the three fractions were significantly higher in demented cases with Alzheimer's disease than in controls but did not significantly differ from those found in high probability mismatches.

Amyloid-β dimers, corresponding to the band detected at 8 kDa, were particularly abundant in the 1% Triton^{TM} X-100 and 2% SDS fractions, and were significantly higher in demented cases with Alzheimer's disease when compared with controls but did not significantly differ from those found in high probability mismatches (Fig. 5B and C). Levels of soluble amyloid-β species were also measured by using a two-site sandwich ELISA that preferentially detects monomers but also amyloid-β oligomers. As shown in Fig. 5D, significantly higher levels of soluble amyloid-β were found in demented cases with Alzheimer's disease compared with controls in Tris-buffered saline and SDS soluble fractions but, in agreement with the data obtained by western blot, no statistically significant differences were demonstrated between high probability mismatches and demented cases with Alzheimer's disease. To further explore these observations, we measured levels of amyloid-β oligomers in the Tris-buffered saline soluble fraction using a specific oligomeric amyloid-β ELISA able to distinguish higher molecular weight amyloid-β assemblies from monomers. As shown in Fig. 5E, this assay detected significantly higher amounts of amyloid-β oligomers in demented cases with Alzheimer's disease

compared with controls but failed to detect differences between high probability mismatches and demented cases with Alzheimer's disease.

We wanted to determine whether levels of soluble amyloid-β peptides segregated into distinct cellular compartments would differentially correlate with cognition and anatomical integrity in the presence of Alzheimer's disease pathology. We prepared synaptic enriched fractions and measured amyloid-β monomers and dimers by western blot using specific antibodies against amyloid-β (Fig. 6B and C). As shown in Fig. 6C levels of amyloid-β monomers and dimers in synaptoneurosomes were significantly higher in demented cases with Alzheimer's disease compared with controls but did not significantly differ from those found in high probability mismatches

In contrast, when we measured oligomeric amyloid-β deposits reactive to NAB61, an antibody that preferentially recognizes a conformational epitope present in dimeric, small oligomeric, and higher order amyloid-β structures but not full-length amyloid-β precursor protein (APP) or C-terminal APP (Lee *et al*., 2006; Koffie *et al*., 2009), we noted a >5-fold higher NAB61 burden in demented cases with Alzheimer's disease than in high probability mismatches (Table 1, Fig. 6D and E). We believe this observation is particularly noteworthy because it suggests that different methods used to assess amyloid-β oligomers likely report different amyloid-β assemblies, thus limiting direct comparison of results from different assays.

The above data indicate that although biochemical measurements of soluble amyloid-β oligomeric species, based on western blot and sensitive ELISA assays, failed to discriminate demented Alzheimer's disease from high probability mismatches, quantitative immunohistochemical assessment using a conformer-specific antibody revealed a close relationship between oligomeric amyloid-β deposits and anatomical derangement in this series.

Aberrant accumulation of soluble phospho-tau species into the synaptic compartment discriminated demented cases with Alzheimer's disease but not high probability mismatches from controls

An alternate or additional possibility we have investigated is that the tau phenotype (soluble tau species versus neurofibrillary tangles) could contribute to explain the resilience of high probability mismatches to Alzheimer's disease pathology. In addition to the pool of insoluble hyperphosphorylated tau contained in classic neurofibrillary tangles in the cell soma, and in dendrites and dystrophic axons nearby fibrillar amyloid plaques, it has been recently proposed that soluble hyperphosphorylated tau species may substantially contribute to impaired cognition in Alzheimer's disease (Berger *et al*., 2007; Lasagna-Reeves *et al*., 2011). We measured levels of soluble tau species in cytosolic and synaptic fractions obtained from samples containing the superior temporal sulcus region by using western blot and specific antibodies against human tau and phospho-tau epitopes. As shown in
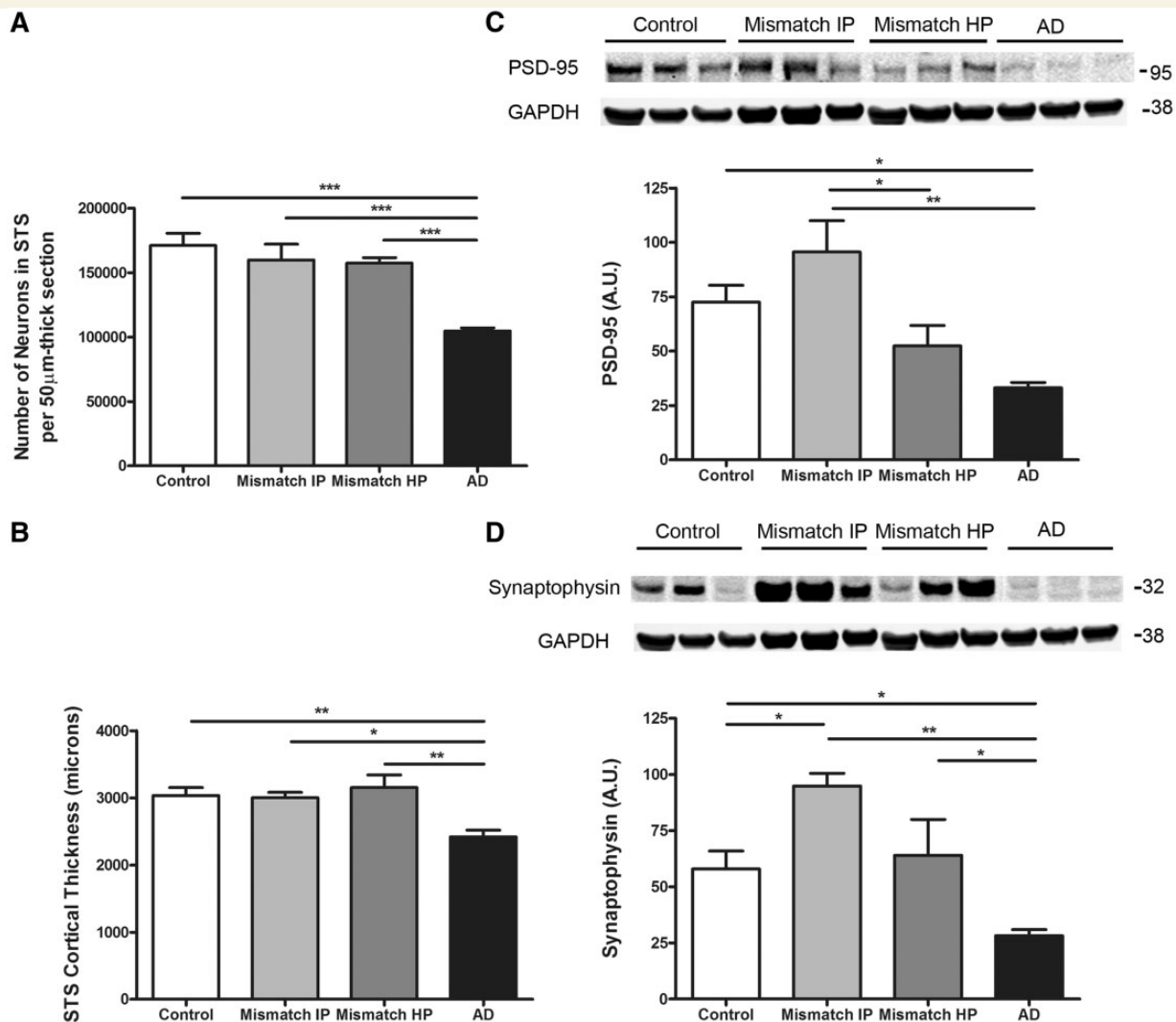
Figure 2 Number of neurons, cortical thickness and synaptic markers in the superior temporal sulcus. (**A**) Stereologically based neuronal counts in the superior temporal sulcus (STS) showed a significant reduction by >40% in the number of neurons in demented cases with Alzheimer's disease (AD) compared to controls. Intermediate (Mismatch IP) and high probability mismatches (Mismatch HP) showed no significant neuronal loss in this region compared with controls. (**B**) Superior temporal sulcus cortical thickness was significantly reduced by >20% in cases with Alzheimer's disease but not in intermediate or high probability mismatches when compared to controls. (**C**) Representative image of western blot and quantification for postsynaptic marker PSD-95. Levels of PSD-95 in the superior temporal sulcus were significantly decreased in cases with Alzheimer's disease but not in intermediate or high probability mismatches when compared with controls. (**D**) Representative image of western blot and quantification for presynaptic marker synaptophysin. Levels of synaptophysin in the superior temporal sulcus were significantly decreased in cases with Alzheimer's disease but not in high probability mismatches when compared with controls. A significantly higher level of synaptophysin was detected in the superior temporal sulcus in intermediate probability mismatches compared with controls. GAPDH was used as loading control. $n = 5$–8 per group; *$P < 0.05$; **$P < 0.01$; ***$P < 0.001$. One way ANOVA and *post hoc* Tukey test.

Fig. 7A and B, the majority of tau in controls and high probability mismatches was found in the cytosolic fraction in the form of monomers whereas in demented cases with Alzheimer's disease soluble tau species preferentially accumulated within the synaptic compartment ranging from monomeric (migrating at ~64 kDa) to high molecular weight multimeric forms (75–250 kDa) and were abnormally hyperphosphorylated (Fig. 7C and D). The levels of hyperphosphorylated tau monomers and multimers in synapses were significantly increased in demented cases with Alzheimer's disease but not in high probability mismatches when compared with controls. Abundant low molecular weight bands (migrating at ~20–50 kDa), likely corresponding to truncated forms of tau, were also observed within the synaptic compartment in demented cases with Alzheimer's disease, but only present in very small quantities or absent in high probability mismatches and controls. These data suggest that aberrant accumulation of soluble hyperphosphorylated tau into synapses might contribute to a greater extent than tangle formation to clinical symptoms and neuronal and synaptic disruption in Alzheimer's disease.
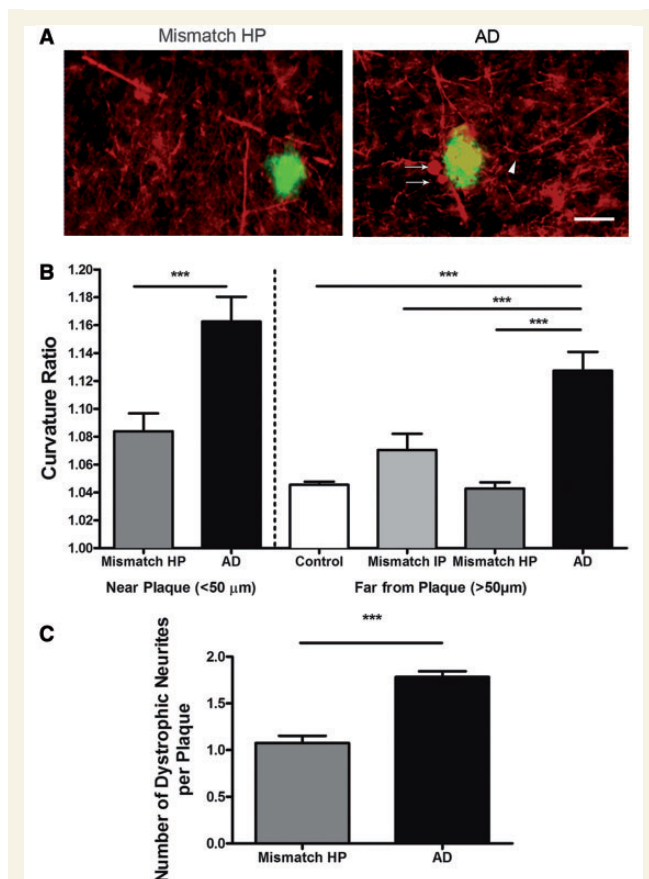
Figure 3 Neurite trajectory analysis. (**A**) Representative photomicrographs of SMI-312 immunostained axons (red) and thioflavin-S labelled amyloid plaques (green) in the superior temporal sulcus. Arrowhead shows example of curved axonal segment. Arrows show examples of neuritic dystrophies. Scale bar = 50 μm. (**B**) Demented cases with Alzheimer's disease (AD) had significantly curvier axons close (<50 μm) and far (>50 μm) from plaque than high and intermediate probability mismatches (Mismatch IP and HP) and controls free of Alzheimer's disease pathology (control); ***$P < 0.001$. Mann Whitney test ('close to plaque' analysis) and Kruskal-Wallis ANOVA and Dunn's multiple comparison test ('far from plaque' analysis). (**C**) The number of dystrophic neurites was significantly higher in cases with Alzheimer's disease compared to high probability mismatches. $n = 172$–290 axonal segments 'close to plaque' and 238–456 axonal segments 'far from plaque'; ***$P < 0.001$ Mann Whitney test.

Number of GFAP-positive astrocytes and CD68-positive microglia is increased in demented cases with Alzheimer's disease but not in high probability mismatches

Abundant activated glia and release of proinflammatory mediators are consistently identified in association with fibrillar thioflavin-S-positive plaques in Alzheimer's disease brains and trangenic mouse models (McGeer and McGeer, 1996, 2007; Wyss-Coray, 2006).
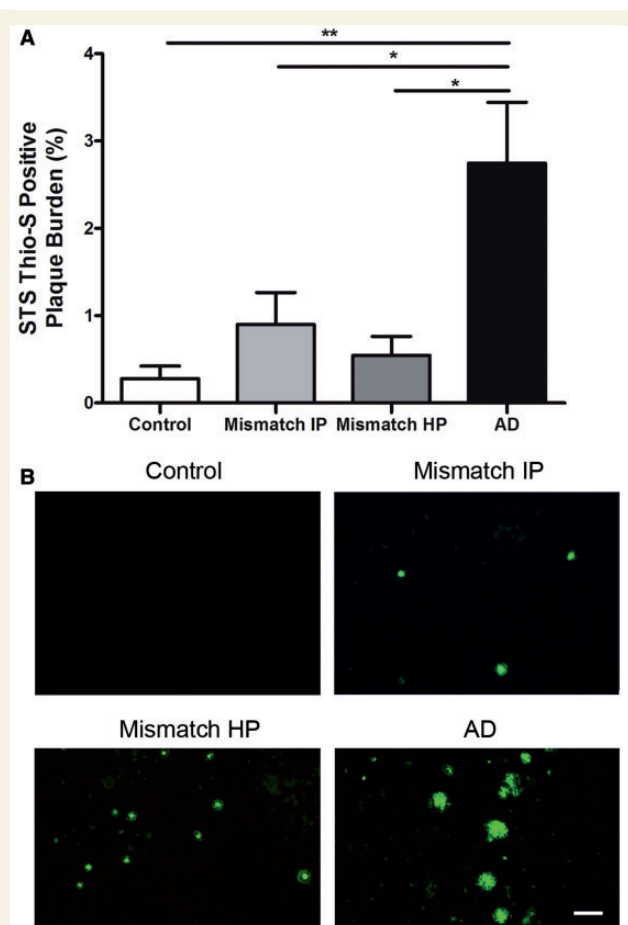

Figure 4 Superior temporal sulcus thioflavin-S-positive amyloid plaque burden. (**A**) Demented cases with Alzheimer's disease (AD) had a significantly higher thioflavin-S-positive plaque burden in the superior temporal sulcus when compared with intermediate and high probability mismatches (Mismatch HP and IP). $n = 8$–10 per group; *$P < 0.05$, **$P < 0.01$. One way ANOVA and *post hoc* Tukey test. (**B**) Representative photomicrographs of thioflavin-S stained plaques in the superior temporal sulcus. Scale bar = 100 μm.

Whether or not glial activation substantially contributes to structural damage and impaired cognition in Alzheimer's disease remains unknown. We performed stereological counts in the superior temporal sulcus of astrocytes stained with an antibody to GFAP, a well-recognized marker of reactive astrocytes, and activated microglial cells stained with an antibody to CD68. We noted a significant increase in the amount of activated astrocytes and microglial cells in demented cases with Alzheimer's disease in comparison with controls but not in intermediate or high probability mismatches (Fig. 8A–D). The robust difference observed in glial cell responses between mismatches and demented cases with Alzheimer's disease suggests that aberrant glial activation might play a deleterious role on neuronal function and integrity in Alzheimer's disease. Alternatively, the lack of activation of these glial elements in mismatches may reflect the relative lack of synaptic and neuronal damage in these cases.
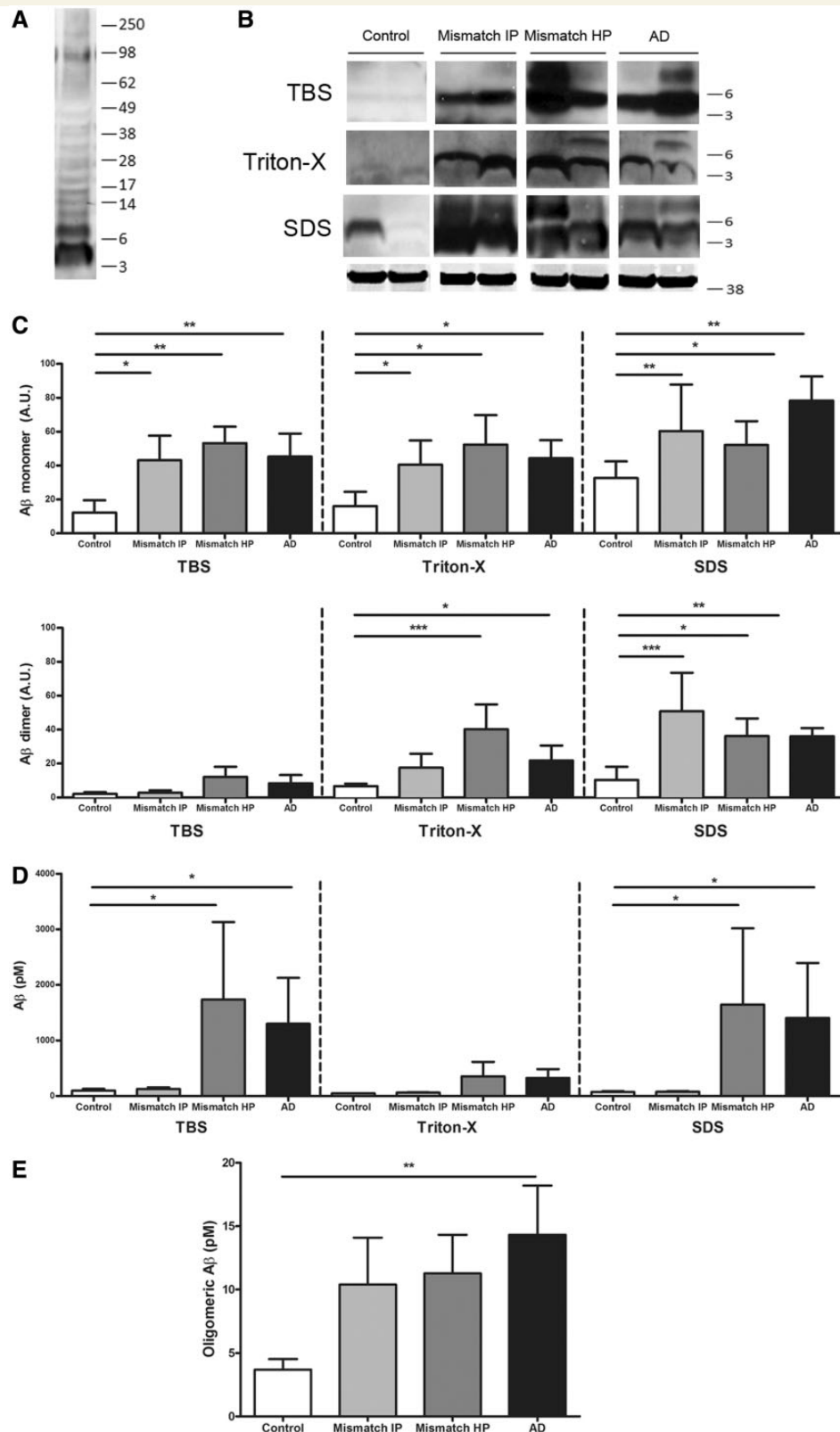
Figure 5 Biochemical analyses of soluble amyloid-β species in serially extracted samples (Tris-buffered saline, 1% Triton™ X-100 and 2% SDS) containing the superior temporal sulcus. (**A**) Representative image of western blot showing bands recognized by 6E10 plus 82E1 antibodies. (**B**) Representative image of western blot for amyloid-β monomers (4 kDa) and dimers (8 kDa); GAPDH (38 kDa) is used as loading control. (**C**) Levels of amyloid-β monomers and dimers by western blot did not significantly differ between demented cases with Alzheimer's disease (AD) and intermediate or high probability mismatches (Mismatch IP and HP) but were significantly higher in all three groups compared to controls (monomers in all three fractions and dimers in Triton™ X-100 and SDS fractions). (**D**) Two-sandwich ELISA

(continued)

Discussion

Increasing evidence suggests that some individuals can tolerate substantial amounts in their brains of classical Alzheimer's disease lesions, e.g. plaques and tangles, without becoming demented (Klunk *et al.*, 2004; Lopresti *et al.*, 2005; Riley *et al.*, 2005; Mintun *et al.*, 2006; Rowe *et al.*, 2007; Aizenstein *et al.*, 2008; Schneider *et al.*, 2009). Although these mismatches are infrequent, their study may prove useful for the design of neuroprotective and cognitive sparing therapies in the elderly. Literature
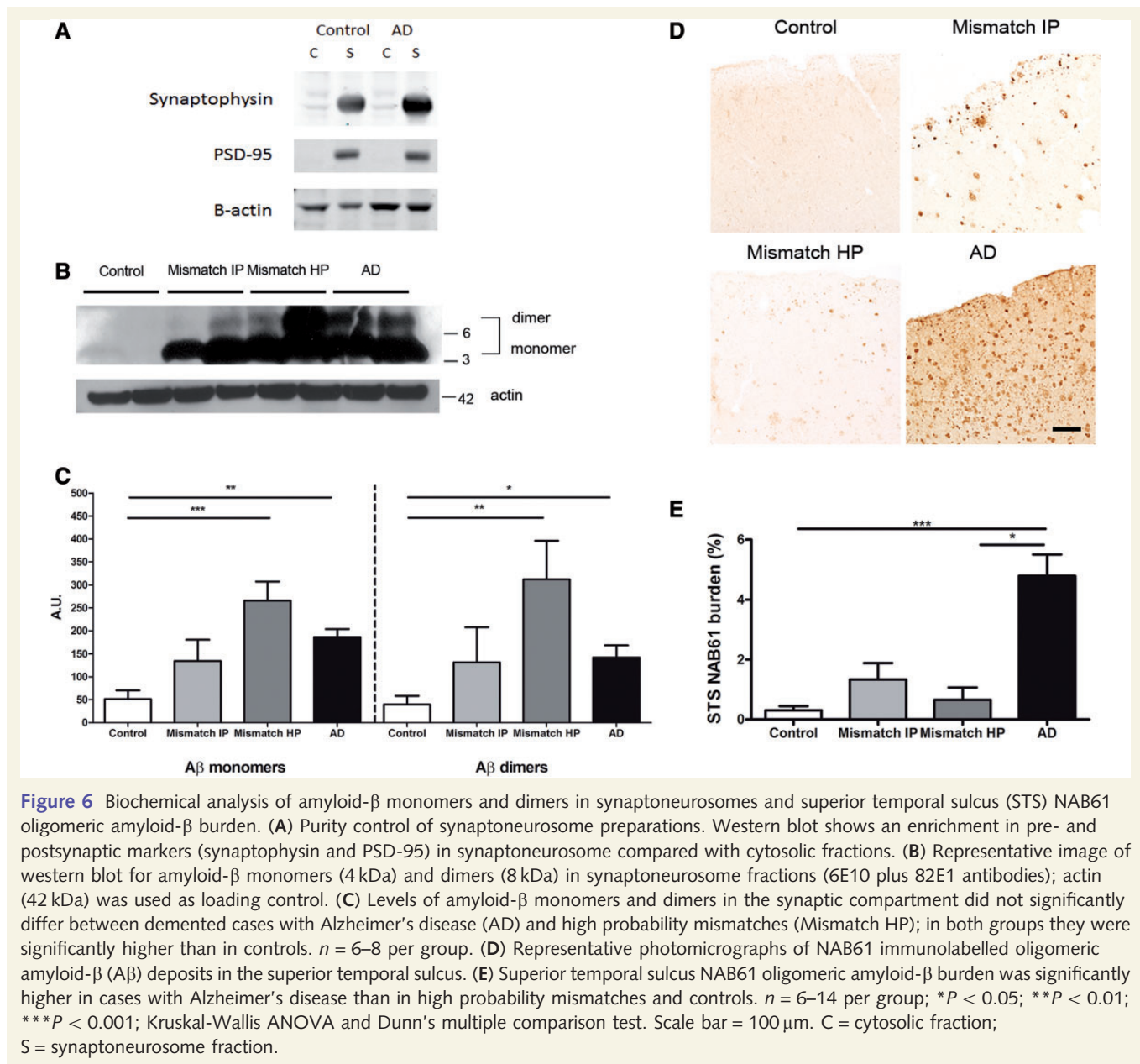

Figure 6 Biochemical analysis of amyloid-β monomers and dimers in synaptoneurosomes and superior temporal sulcus (STS) NAB61 oligomeric amyloid-β burden. (**A**) Purity control of synaptoneurosome preparations. Western blot shows an enrichment in pre- and postsynaptic markers (synaptophysin and PSD-95) in synaptoneurosome compared with cytosolic fractions. (**B**) Representative image of western blot for amyloid-β monomers (4 kDa) and dimers (8 kDa) in synaptoneurosome fractions (6E10 plus 82E1 antibodies); actin (42 kDa) was used as loading control. (**C**) Levels of amyloid-β monomers and dimers in the synaptic compartment did not significantly differ between demented cases with Alzheimer's disease (AD) and high probability mismatches (Mismatch HP); in both groups they were significantly higher than in controls. $n = 6$–8 per group. (**D**) Representative photomicrographs of NAB61 immunolabelled oligomeric amyloid-β (Aβ) deposits in the superior temporal sulcus. (**E**) Superior temporal sulcus NAB61 oligomeric amyloid-β burden was significantly higher in cases with Alzheimer's disease than in high probability mismatches and controls. $n = 6$–14 per group; $*P < 0.05$; $**P < 0.01$; $***P < 0.001$; Kruskal-Wallis ANOVA and Dunn's multiple comparison test. Scale bar = 100 μm. C = cytosolic fraction; S = synaptoneurosome fraction.

Figure 5 Continued

using BNT77/BA27 antibody pair did not detect significant differences in soluble amyloid-β levels (monomers and oligomers) between cases with Alzheimer's disease and high probability mismatches; in both groups amyloid-β levels were significantly higher in Tris-buffered saline and SDS fractions than in intermediate probability mismatches and controls. (**E**) Same site sandwich ELISA (82E1), specific for dimers and higher molecular weight amyloid-βspecies, did not detect significant differences between Alzheimer's disease and high probability mismatches; Alzheimer's disease had significantly higher levels of oligomeric amyloid-β than controls. $n = 7$–11 per group; $*P < 0.05$; $**P < 0.01$; $***P < 0.001$; Kruskal-Wallis ANOVA and Dunn's multiple comparison test.
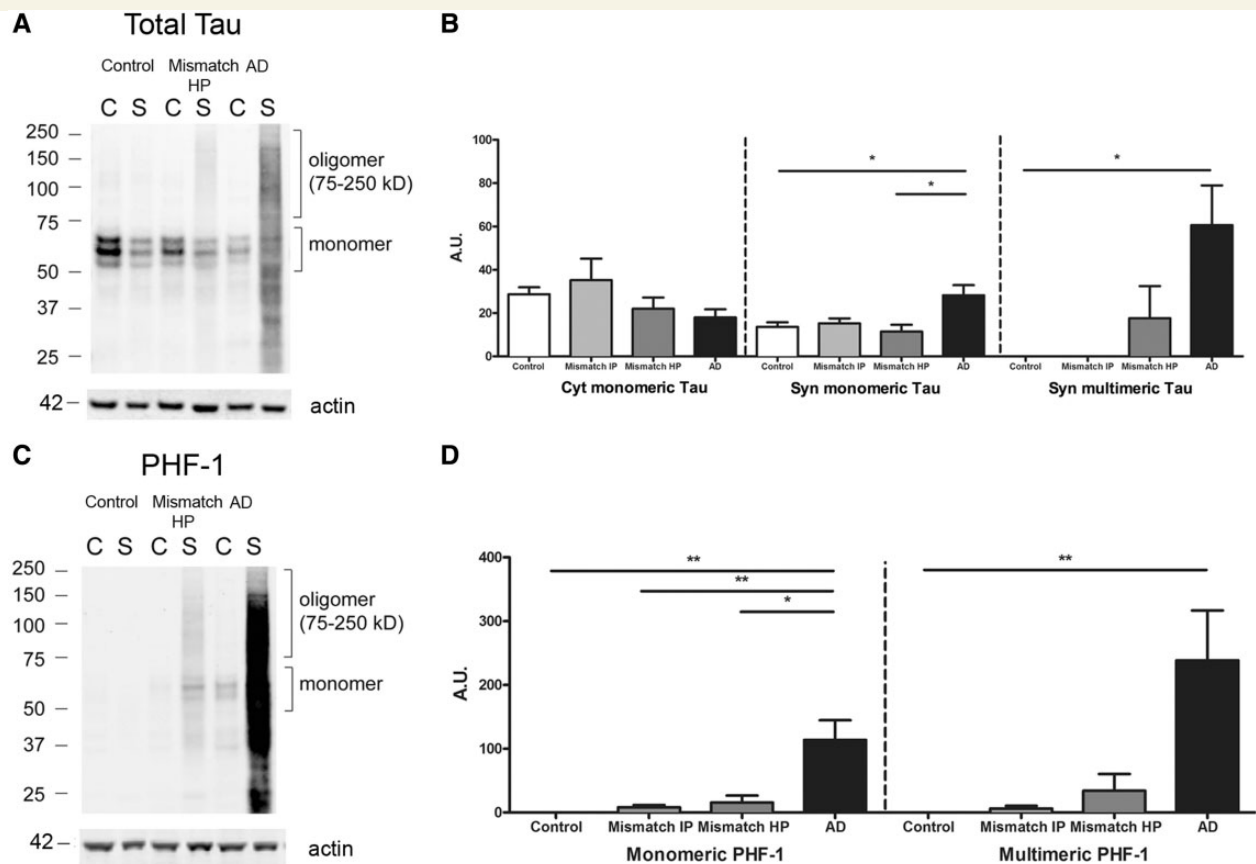
Figure 7 Biochemical analysis of total tau and hyperphosphorylated monomeric and multimeric tau in synaptoneurosomes. (**A**) Representative images of cytosolic (C) and synaptoneurosome (S) fractions on western blot for total human tau (H7 antibody) and (**C**) hyperphosporylated tau (PHF-1 antibody), showing strong accumulation of tau monomers and multimers at synapses in demented Alzheimer's disease (AD) cases. (**B**) Quantitative analyses for (C) cytosolic and (S) synaptic total tau and (**D**) hyperphosphorylated tau showed selective and significantly higher accumulation of monomeric tau (64 kDa) and multimeric tau (75-250 kDa) species in synapses in cases with Alzheimer's disease, but not in intermediate and high probability mismatches (Mismatch IP and HP) when compared with controls. Total levels of tau monomers in the cytosol did not significantly differ between groups. Actin (42 kDa) was used as loading control. $n = 6–9$ per group; $*P < 0.05$; $**P < 0.01$; Kruskal-Wallis ANOVA and Dunn's multiple comparison test.

concerning these unique cases, apparently resilient to Alzheimer's disease pathology, is scarce and fundamental questions remain unanswered. For instance, it is unclear whether the load of Alzheimer's disease pathological lesions in mismatches, when carefully quantified, is comparable to that found in cases with Alzheimer's disease with dementia. Thus, the most parsimonious explanation for the absence of dementia in these cases would be that their plaque and tangle burdens are substantially lower than in demented cases with Alzheimer's disease. Alternatively, despite the accumulation of equivalent amounts of plaques and tangles, some brains may be nonetheless resilient to structural damage assessed in terms of neuronal and synaptic loss, and neuropil disruption. And in this case, the possibility exists that one or more pathological species other than classical tangles or plaques might correlate better with structural brain damage and the consequent neuronal system collapse. For example, recent data have suggested that soluble forms of amyloid-β and tau may play a much larger role in synapse and neuronal damage and clinical symptoms of dementia than plaques and tangles themselves

(Selkoe, 1991; Shankar et al., 2008; De Calignon et al., 2010; McDonald et al., 2012).

Our data support the idea that amyloid-β plaque deposition and tangle formation do not inevitably result in dementia in all individuals. Although an insufficient load of plaques and tangles in the neocortex may explain the absence of dementia in mismatches pathologically classified as intermediate probability of Alzheimer's disease, a rare subset of apparently non-demented individuals that could be classified as high probability of Alzheimer's disease by NIA-RI criteria was identified in this series. Detailed quantitative assessments demonstrated that these high probability mismatches were well matched to demented cases with Alzheimer's disease with regards to amyloid-β plaques and neurofibrillary tangles in the superior temporal sulcus, therefore, we feel these cases represent individuals who seem resistant to Alzheimer's disease pathology. If these cases simply had greater 'reserve' of neurons and synapses, one would expect equivalent degrees of local damage around plaques and equally robust glial inflammatory changes. This was not the case. Instead, further detailed pathological
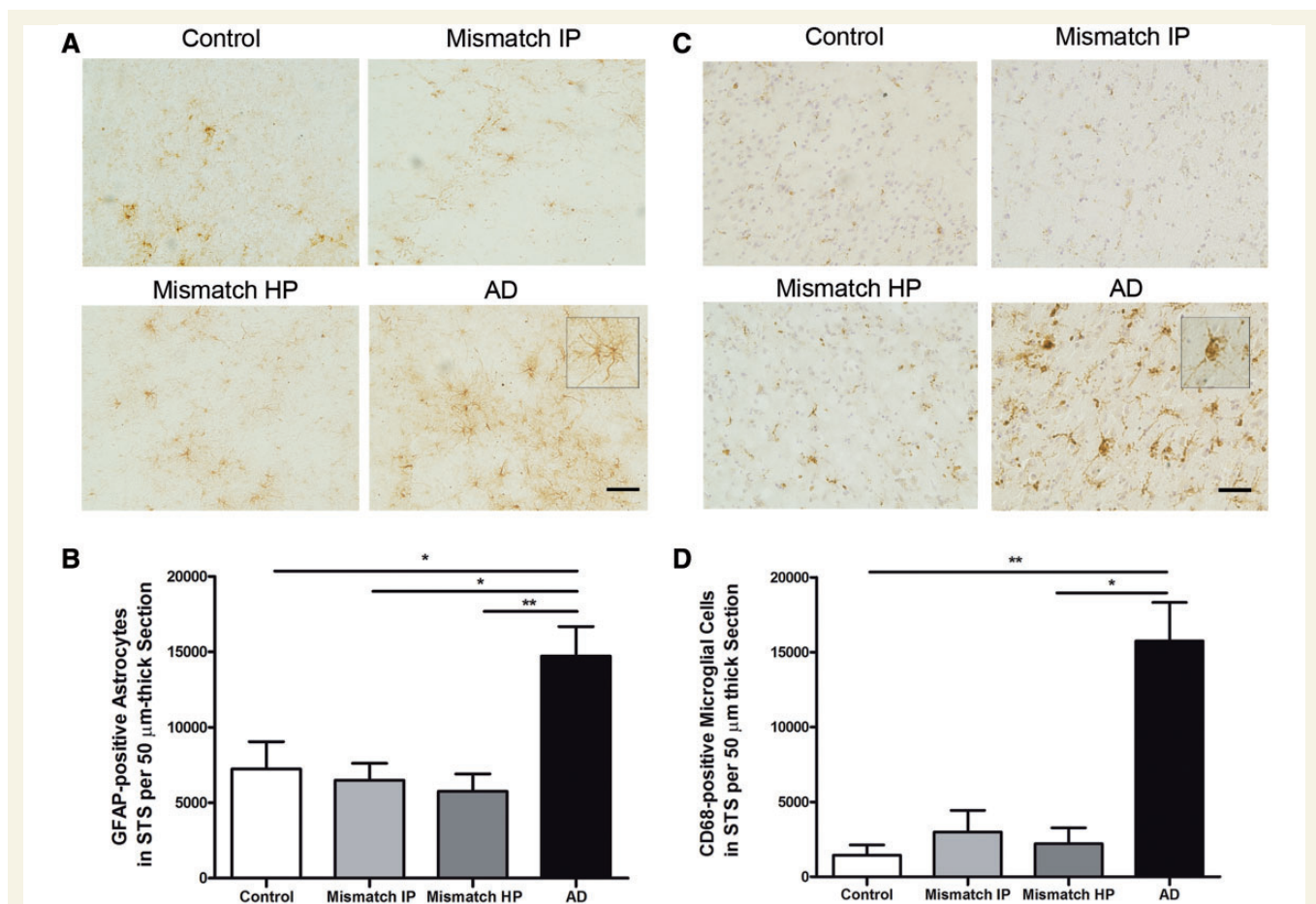
Figure 8 Number of GFAP-positive astrocytes in the superior temporal sulcus and CD68-positive microglia. (**A**) Representative photomicrographs of GFAP-positive astrocytes. (**B**) Stereological counts of astrocytes in the superior temporal sulcus (STS) on sections immunostained with GFAP showed a significant increase in the amount of GFAP-positive astrocytes in demented cases with Alzheimer's disease but not in intermediate probability (Mismatch IP) or high probability mismatches (Mismatch HP) in comparison with controls. (**C**) Representative photomicrographs of CD68-positive microglia cells in the superior temporal sulcus. Haematoxylin was used as a counterstain. (**D**) Stereological counts of microglia in the superior temporal sulcus on sections immunostained with CD68 showed a significant increase in the amount of CD68-positive microglial cells in demented cases with Alzheimer's disease, but not in intermediate or high probability mismatches in comparison with controls. $n = 8$–14 per group; *$P < 0.05$; **$P < 0.01$. One way ANOVA and *post hoc* Tukey test, and Kruskal-Wallis ANOVA and Dunn's multiple comparison test, respectively. Scale bar = 100 μm.

characterization of these cases provided evidence that their neuronal populations and the morphology of their neurites were remarkably well preserved in comparison with the massive neuronal depopulation and the dramatic distortion of neurite architecture seen in demented cases with Alzheimer's disease. A differential phenotype characterized by a larger cortical load of fibrillar thioflavin-S-reactive plaques and oligomeric amyloid-β deposits labelled by a conformer-specific antibody, aberrant accumulation of hyperphosphorylated soluble tau at synapses and a robust glial cell response differentiated demented cases with Alzheimer's disease from high probability mismatches, pointing to those factors as potential mediators of neurotoxicity and impaired cognition in Alzheimer's disease.

One caveat in our study is that formal neuropsychological evaluation close to death was not available in all cases. Thus, although dementia was not reported in any of the controls or

mismatches, subtle declines in cognition cannot be unequivocally ruled out in some of the cases. However, it should be acknowledged that a high load of Alzheimer's disease pathology in cortical association areas like the superior temporal sulcus is expected to be associated with robust cognitive deficits sufficient to meet criteria for dementia. Thus, we feel confident that cognition in our non-demented mismatches was, being conservative, much better preserved than in demented cases with Alzheimer's disease with a comparable load of Alzheimer's disease pathology in the neocortex.

Studies addressing whether the number of neurons and synapses in subjects with Alzheimer's disease pathology but preserved cognition are comparable to age-matched control subjects free of Alzheimer's disease pathology or substantially decreased are very limited. In a recent study, neuronal densities and pre- and post-synaptic elements in the midfrontal gyrus were found to be

preserved in cognitively normal subjects with high burden of Alzheimer's disease pathology compared with controls free of Alzheimer's disease pathology (Arnold *et al.*, 2013). Of note, in that study no significant decrease in neuronal density was detected in demented cases with Alzheimer's disease. A significant hypertrophy of neuronal cell bodies, nuclei and nucleoli was reported in the cortex and the CA1 region in clinically asymptomatic subjects with Alzheimer's disease pathology from the Nun Study, and it was hypothesized that it might represent an early brain reaction to the presence of plaques and tangles, or a compensatory mechanism that prevents clinical progression to dementia (Iacono *et al.*, 2008, 2009). Our study corroborates that there is neither neuronal loss nor significant decrease of pre- or postsynaptic markers in the superior temporal sulcus of mismatches with neuropathologically high probability of Alzheimer's disease in comparison with similarly aged controls free of substantial classical Alzheimer's disease pathology. As discussed below, the finding of robust differences between these mismatches and demented cases with Alzheimer's disease in the alteration of axonal morphology around plaques and in glial activation argues against a natural protection of mismatches against dementia due to a higher baseline number of neurons and synapses compared with average individuals.

In Alzheimer's disease brains amyloid-β plaques appear in a variety of morphological forms including 'diffuse' plaques, immunoreactive deposits of amyloid-β that do not appear to have a substantial effect on the neuropil and do not incite a glial response, and 'neuritic' plaques that in general contain a core of amyloid that can be stained with dyes like thioflavin-S, and that are surrounded by disruption in the neuropil, local glial activation, and often dystrophic axons and dendrites that contribute to their neuritic component (Dickson and Vickers, 2001). Multiple studies have shown that total amyloid-β plaque load does not correlate well with cognitive impairment in demented subjects with Alzheimer's disease (Arriagada *et al.*, 1992; Gomez-Isla *et al.*, 1997) and numerous diffuse plaques may be present in limbic and neocortical regions in cognitively normal individuals (Arriagada *et al.*, 1992; Morris *et al.*, 1996; Knopman *et al.*, 2003). Our data show similar burdens in the superior temporal sulcus of total amyloid-β plaques in high probability mismatches and demented cases with Alzheimer's disease but a significantly larger load and size of fibrillar thioflavin-S-positive plaques in demented cases further suggesting that this particular subset of plaques is more closely related to dementia and neuronal loss in Alzheimer's disease. Detailed analyses of axonal morphology in this series confirmed a robust distortion of neurite morphology in demented cases with Alzheimer's disease as previously reported (Arriagada *et al.*, 1992; Knowles *et al.*, 1999; Le *et al.*, 2001; Spires *et al.*, 2005). Neurite changes were especially severe close to fibrillar amyloid-β plaques, but could also be demonstrated far from them. Interestingly, the trajectory and morphology of axons was much better preserved in high probability mismatches than in demented cases with Alzheimer's disease, even near plaques. Of note, this cannot be attributed to the smaller average plaque size noted in high probability mismatches as previous studies demonstrated that the higher curvature ratio of axons observed close to plaques is not influenced by the size of the plaque (Serrano-Pozo

et al., 2010). The finding of a relatively spared neurite geometry in high probability mismatches in comparison to demented cases with Alzheimer's disease has two important implications. First, it reinforces the idea that these widespread neurite alterations represent a substantial additional type of lesion in Alzheimer's disease that likely contributes to dementia. And second, it suggests that factors other than the toxic effect of fibrillar amyloid-β deposits themselves, and that are intimately related to them (e.g. oligomeric amyloid-β accrual inside and around plaques and glial cell reaction) may likely contribute to alter the geometry and morphology of neurites in Alzheimer's disease.

The idea that soluble species of amyloid-β ('amyloid-β oligomers'), rather than or in addition to plaques, could be the toxic moiety in Alzheimer's disease brains resolving the central paradox in the field of the lack of correlation between amyloid-β deposits and clinical symptoms or neuronal cell loss has recently gained attention (Selkoe, 1991). Amyloid-β dimers, in particular, directly isolated from Alzheimer's disease brains were reported to impair synaptic plasticity and memory in rodents (Shankar *et al.*, 2008). Some recent studies in humans have suggested that soluble amyloid-β oligomers strongly correlate with cognitive impairment in Alzheimer's disease (Tomic *et al.*, 2009; McDonald *et al.*, 2012). Another study recently reported a weaker correlation of the ratio of amyloid-β oligomers to plaque density in non-demented individuals with high brain plaque burden than in demented cases with Alzheimer's disease (Esparza *et al.*, 2013). However, concerns have been raised regarding difficulties in interpreting and comparing data from different laboratories in the absence of consensus on the exact meaning of the term 'toxic amyloid-β oligomer', the likely existence of a mixture of different species in the amyloid-β oligomeric fractions isolated from human brains, and the lack of a common validated technique to measure amyloid-β oligomers (Benilova *et al.*, 2012). In the present study, biochemical assessments of brain soluble amyloid-β species—monomers, dimers and higher molecular weight assemblies—by western blot and sensitive and specific amyloid-β oligomeric ELISA assays confirmed the presence of significantly higher levels of these species in demented cases with Alzheimer's disease compared with controls, but we could not detect significant differences between high probability mismatches and demented cases. Only when we used immunohistochemistry and a conformer-specific antibody (NAB61), we found a significantly higher burden of oligomeric amyloid-β deposits in demented Alzheimer's disease than in high probability mismatches. NAB61-positive amyloid-β oligomeric deposits were mainly seen decorating the periphery and core of fibrillar plaques, as noted in previous human and mouse studies (Koffie *et al.*, 2009; DaRocha-Souto *et al.*, 2011; Koffie *et al.*, 2012). Of note, NAB61 was effective in normalizing cognition in immunotherapy experiments in transgenic mice suggesting that it can detect neurotoxic amyloid-β species (Lee *et al.*, 2006). Several explanations may reconcile these apparently conflicting results derived from biochemical and immunohistological assessments of amyloid-β oligomers in our series. One possibility is that amyloid-β oligomers recognized by NAB61 might represent a 'toxic' but relatively small fraction of the mixture of soluble amyloid-β species detected by western blot and ELISA assays, as different techniques and antibodies may report different amyloid-β assemblies. It is also

possible that a large proportion of the amyloid-β oligomeric species detected by these biochemical methods might not be naturally occurring in the human brain, but rather be artificially promoted by the extracting technique as recently suggested by others (Watt *et al.*, 2013). In this scenario, the development and validation of analytical tools that reliably measure amyloid-β oligomers in the CSF should help solve these critical uncertainties.

Alternatively, or in addition to soluble forms of amyloid-β, soluble species of tau could play a substantial role in neural system disruption and altered cognition in Alzheimer's disease. Our previous studies (Gomez-Isla *et al.*, 1996, 1997) demonstrated that, although total number of tangles strongly predicts number of neurons lost in Alzheimer's disease brains, the amount of neuronal loss outstrips tangle formation by at least one order of magnitude (Gomez-Isla *et al.*, 1997), suggesting that there are likely non-tangle-related mechanisms responsible for neuronal death in Alzheimer's disease. In support of this idea, potentially toxic multimeric tau species were found to strongly correlate with memory loss in brain samples from tau transgenic mice and from patients with Alzheimer's disease and frontotemporal dementia and parkinsonism linked to chromosome 17 (Berger *et al.*, 2007). Moreover, recent studies using *in vivo* multiphoton imaging to observe how tangles form in living tau transgenic mice have shown that caspase activation cleaves tau to initiate tangle formation, but surprisingly, tangle-bearing neurons are long-lived, further favouring the idea that tangles are 'off pathway' to acute neuronal death, and that soluble tau species, rather than tangles, might be the critical toxic moiety underlying neurodegeneration (De Calignon *et al.*, 2010). We have recently shown that, in addition to its well-described axonal localization, normal soluble tau is also present at both presynaptic and postsynaptic terminals in control brains; and synaptic tau becomes hyperphosphorylated and ubiquitinated, and forms stable multimeric assemblies resistant to SDS denaturation in Alzheimer's disease brains (Tai *et al.*, 2012). Here we provide further evidence of an aberrant accrual of soluble monomeric and multimeric species of hyperphosphorylated tau within the synaptic compartment in demented cases with Alzheimer's disease but not in high probability mismatches in comparison with controls. If confirmed in future studies, this would favour the idea that abnormal accumulation of soluble tau species into synapses might be more directly related to neuronal damage and dementia than classic tangles. Of note, the presence of mistargeted soluble tau forms at synapses in demented cases with Alzheimer's disease would argue in favour of the recently suggested neuron-to-neuron propagation of tau pathology in a murine model of early Alzheimer's disease (De Calignon *et al.*, 2012; Liu *et al.*, 2012).

Aside from differences in the amyloid-β and tau phenotypes, one of the most striking phenotypic divergences observed in high probability mismatches was the lack of glial activation when compared to demented cases. Although brain inflammation is thought to be an important factor in Alzheimer's disease, how and to what extent it may contribute to synaptic and neuronal damage and altered cognition in Alzheimer's disease remains unknown. In Alzheimer's disease brains glial responses were found to increase linearly with progression of the disease around plaques and tangles (Serrano-Pozo *et al.*, 2011). Two

large genome-wide association studies (Harold *et al.*, 2009; Lambert *et al.*, 2009) have identified receptor for complement C3b, a key regulator of complement activation, as one of the genes that increases the risk for late-onset Alzheimer's disease. More recently, a rare variant in the gene encoding TREM2 (triggering receptor expressed on myeloid cells 2), that is expressed in microglial cells, was found to confer a significant risk of Alzheimer's disease (Jonsson *et al.*, 2013) further supporting the importance of inflammatory mechanisms in Alzheimer's disease. In transgenic mice, the number of GFAP-positive astrocytes was the parameter most closely correlated with memory impairment and neuronal cell loss (DaRocha-Souto *et al.*, 2011), and treatment with triflusal—an anti-inflammatory drug that inhibits NF-κB activation—significantly decreased glial activation and rescued alterations in neurite morphology and memory deficits despite lack of reduction of amyloid-β plaque burden (Coma *et al.*, 2010). The above data and the findings reported here favour the idea that aberrant activation of glial elements, rather than reflecting a mere response to neuronal injury, may substantially contribute to neuronal cell damage and neurite changes in Alzheimer's disease. Whether or not glial cell response influences amyloid-β and tau oligomerization/fibrillation and/or neuronal propagation of altered forms of amyloid-β and tau remains unknown. In humans, the expression of an innate pro-inflammatory cytokine profile in middle age offspring with parental history of late-onset Alzheimer's disease was identified as a risk factor of Alzheimer's disease in old age (Van Exel *et al.*, 2009) suggesting that inflammation in early years may contribute to development of Alzheimer's disease pathology and cognitive impairment later in life. In a recent study in mice the use of an adeno-associated viral vector to drive selective astrocyte expression of VIVIT, a peptide that interferes with the inflammatory calcineurin/nuclear factor of activated T cells signalling pathway, improved cognition and decreased glial activation and amyloid levels (Furman *et al.*, 2012). Thus, it is possible that a toxic gain of function and/or the loss of physiological neuroprotective functions of glial cells in the neocortex of demented cases with Alzheimer's disease may account in part for the larger brain accrual of fibrillar amyloid-β plaques and oligomeric amyloid-β deposits, the aberrant accumulation of hyperphoshorylated soluble tau in synapses, and the striking loss of neurons and synaptic markers seen in these cases in comparison to high probability mismatches. Further studies directed at the role of glia in neurodegeneration and altered cognition in Alzheimer's disease are now needed.

In conclusion, our study suggests that some unique individuals can tolerate a high burden of amyloid-β plaques and tangles without experiencing dementia or a substantial disruption in neuronal integrity and neurite architecture. Detailed biochemical and histopathological analyses of such cases selectively identified enhanced accrual of amyloid-β in the form of fibrillar plaques and intimately related oligomeric amyloid-β deposits, accumulation of soluble hyperphosphorylated tau in synapses, and aberrant glial cell reaction as likely mediators of neurotoxicity and altered cognition in Alzheimer's disease, providing further insight into factors and pathways potentially involved in human resilience to Alzheimer's disease pathology.

Acknowledgements

Funding

References

Aizenstein HJ, Nebes RD, Saxton JA, Price JC, Mathis CA, Tsopelas ND, et al. Frequent amyloid deposition without significant cognitive impairment among the elderly. Arch Neurol 2008; 65: 1509–17.

Arias E. United States life tables, 2008. Natl Vital Stat Rep 2012; 61: 3.

Arnold SE, Louneva N, Cao K, Wang LS, Han LY, Wolk DA, et al. Cellular, synaptic, and biochemical features of resilient cognition in Alzheimer's disease. Neurobiol Aging 2013; 34: 157–68.

Arriagada PV, Marzloff K, Hyman BT. Distribution of Alzheimer-type pathologic changes in nondemented elderly individuals matches the pattern in Alzheimer's disease. Neurology 1992; 42: 1681–88.

Benilova I, Karran E, De SB. The toxic Abeta oligomer and Alzheimer's disease: an emperor in need of clothes. Nat Neurosci 2012; 15: 349–57.

Berger Z, Roder H, Hanna A, Carlson A, Rangachari V, Yue M, et al. Accumulation of pathological tau species and memory loss in a conditional model of tauopathy. J Neurosci 2007; 27: 3650–62.

Coma M, Sereno L, Da Rocha-Souto B, Scotton TC, España J, Sánchez MB, et al. Triflusal reduces dense-core plaque load, associated axonal alterations and inflammatory changes, and rescues cognition in a transgenic mouse model of Alzheimer's disease. Neurobiol Dis 2010; 38: 482–91.

D'Amore JD, Kajdasz ST, McLellan ME, Bacskai BJ, Stern EA, Hyman BT. In vivo multiphoton imaging of a transgenic mouse model of Alzheimer disease reveals marked thioflavine-S-associated alterations in neurite trajectories. J Neuropathol Exp Neurol 2003; 62: 137–45.

DaRocha-Souto B, Coma M, Perez-Nievas BG, Scotton TC, Siao M, Sánchez-Ferrer P, et al. Activation of glycogen synthase kinase-3 beta mediates beta-amyloid induced neuritic damage in Alzheimer's disease. Neurobiol Dis 2012; 45: 425–37.

DaRocha-Souto B, Scotton TC, Coma M, Serrano-Pozo A, Hashimoto T, Serenó L, et al. Brain oligomeric beta-amyloid but not total amyloid plaque burden correlates with neuronal loss and astrocyte inflammatory response in amyloid precursor protein/tau transgenic mice. J Neuropathol Exp Neurol 2011; 70: 360–76.

De Calignon CA, Fox LM, Pitstick R, Carlson GA, Bacskai BJ, Spires-Jones TL, et al. Caspase activation precedes and leads to tangles. Nature 2010; 464: 1201–04.

De Calignon CA, Polydoro M, Suarez-Calvet M, William C, Adamowicz DH, Kopeikina KJ, et al. Propagation of tau pathology in a model of early Alzheimer's disease. Neuron 2012; 73: 685–97.

Dekosky ST, Scheff SW. Synapse loss in frontal cortex biopsies in Alzheimer's disease: correlation with cognitive severity. Ann Neurol 1990; 27: 457–64.

Dickson TC, Vickers JC. The morphological phenotype of beta-amyloid plaques and associated neuritic changes in Alzheimer's disease. Neuroscience 2001; 105: 99–107.

Esparza TJ, Zhao H, Cirrito JR, Cairns NJ, Bateman RJ, Holtzman DM, et al. Amyloid-beta oligomerization in Alzheimer dementia versus high-pathology controls. Ann Neurol 2013; 73: 104–19.

Furman JL, Sama DM, Gant JC, Beckett TL, Murphy MP, Bachstetter AD, et al. Targeting astrocytes ameliorates neurologic changes in a mouse model of Alzheimer's disease. J Neurosci 2012; 32: 16129–40.

Giannakopoulos P, Herrmann FR, Bussiere T, Bouras C, Kövari E, Perl DP, et al. Tangle and neuron numbers, but not amyloid load, predict cognitive status in Alzheimer's disease. Neurology 2003; 60: 1495–1500.

Gomez-Isla T, Hollister R, West H, Mui S, Growdon JH, Petersen RC, et al. Neuronal loss correlates with but exceeds neurofibrillary tangles in Alzheimer's disease. Ann Neurol 1997; 41: 17–24.

Gomez-Isla T, Price JL, McKeel DW Jr., Morris JC, Growdon JH, Hyman BT. Profound loss of layer II entorhinal cortex neurons occurs in very mild Alzheimer's disease. J Neurosci 1996; 16: 4491–500.

Gomez-Isla T, Spires T, De Calignon A, Hyman BT. Neuropathology of Alzheimer's disease. Handb Clin Neurol 2008; 89: 233–43.

Hampton DW, Webber DJ, Bilican B, Goedert M, Spillantini MG, Chandran S. Cell-mediated neuroprotection in a mouse model of human tauopathy. J Neurosci 2010; 30: 9973–83.

Harold D, Abraham R, Hollingworth P, Sims R, Gerrish A, Hamshere ML, et al. Genome-wide association study identifies variants at CLU and PICALM associated with Alzheimer's disease. Nat Genet 2009; 41: 1088–93.

Hashimoto T, Serrano-Pozo A, Hori Y, Adams KW, Takeda S, Banerji AO, et al. Apolipoprotein E, especially apolipoprotein E4, increases the oligomerization of amyloid beta peptide. J Neurosci 2012; 32: 15181–92.

Iacono D, Markesbery WR, Gross M, Pletnikova O, Rudow G, Zandi P, et al. The Nun study: clinically silent AD, neuronal hypertrophy, and linguistic skills in early life. Neurology 2009; 73: 665–73.

Iacono D, O'Brien R, Resnick SM, Zonderman AB, Pletnikova O, Rudow G, et al. Neuronal hypertrophy in asymptomatic Alzheimer disease. J Neuropathol Exp Neurol 2008; 67: 578–89.

Ikonomovic MD, Klunk WE, Abrahamson EE, Mathis CA, Price JC, Tsopelas ND, et al. Post-mortem correlates of in vivo PiB-PET amyloid imaging in a typical case of Alzheimer's disease. Brain 2008; 131: 1630–45.

Irizarry MC, Soriano F, McNamara M, Page KJ, Schenk D, Games D, et al. Abeta deposition is associated with neuropil changes, but not with overt neuronal loss in the human amyloid precursor protein V717F (PDAPP) transgenic mouse. J Neurosci 1997; 17: 7053–9.

Jonsson T, Stefansson H, Steinberg S, Jonsdottir I, Jonsson PV, Snaedal J, et al. Variant of TREM2 associated with the risk of Alzheimer's disease. N Engl J Med 2013; 368: 107–16.

Klunk WE, Engler H, Nordberg A, Wang Y, Blomqvist G, Holt DP, et al. Imaging brain amyloid in Alzheimer's disease with Pittsburgh Compound-B. Ann Neurol 2004; 55: 306–19.

Knopman DS, Boeve BF, Petersen RC. Essentials of the proper diagnoses of mild cognitive impairment, dementia, and major subtypes of dementia. Mayo Clin Proc 2003; 78: 1290–308.

Knowles RB, Wyart C, Buldyrev SV, Cruz L, Urbanc B, Hasselmo ME, et al. Plaque-induced neurite abnormalities: implications for disruption of neural networks in Alzheimer's disease. Proc Natl Acad Sci USA 1999; 96: 5274–9.

Koffie RM, Hashimoto T, Tai HC, Kay KR, Serrano-Pozo A, Joyner D, et al. Apolipoprotein E4 effects in Alzheimer's disease are mediated by synaptotoxic oligomeric amyloid-beta. Brain 2012; 135: 2155–68.

Koffie RM, Meyer-Luehmann M, Hashimoto T, Adams KW, Mielke ML, Garcia-Alloza M, et al. Oligomeric amyloid beta associates with post-synaptic densities and correlates with excitatory synapse loss near senile plaques. Proc Natl Acad Sci USA 2009; 106: 4012–7.

Lambert JC, Schraen-Maschke S, Richard F, Fievet N, Rouaud O, Berr C, et al. Association of plasma amyloid beta with risk of dementia: the prospective Three-City Study. Neurology 2009; 73: 847–53.

Lasagna-Reeves CA, Castillo-Carranza DL, Sengupta U, Clos AL, Jackson GR, Kayed R. Tau oligomers impair memory and induce synaptic and mitochondrial dysfunction in wild-type mice. Mol Neurodegener 2011; 6: 39.

Le R, Cruz L, Urbanc B, Knowles RB, Hsiao-Ashe K, Duff K, et al. Plaque-induced abnormalities in neurite geometry in transgenic models of Alzheimer disease: implications for neural system disruption. J Neuropathol Exp Neurol 2001; 60: 753–8.

Lee EB, Leng LZ, Zhang B, Kwong L, Trojanowski JQ, Abel T, et al. Targeting amyloid-beta peptide (Abeta) oligomers by passive immunization with a conformation-selective monoclonal antibody improves learning and memory in Abeta precursor protein (APP) transgenic mice. J Biol Chem 2006; 281: 4292–9.

Liu L, Drouet V, Wu JW, Witter MP, Small SA, Clelland C, et al. Trans-synaptic spread of tau pathology *in vivo*. PLoS One 2012; 7: e31302.

Lockhart A, Lamb JR, Osredkar T, Sue LI, Joyce JN, Ye L, et al. PIB is a non-specific imaging marker of amyloid-beta (Abeta) peptide-related cerebral amyloidosis. Brain 2007; 130: 2607–15.

Lopresti BJ, Klunk WE, Mathis CA, Hoge JA, Ziolko SK, Lu X, et al. Simplified quantification of Pittsburgh Compound B amyloid imaging PET studies: a comparative analysis. J Nucl Med 2005; 46: 1959–72.

Mc Donald JM, Savva GM, Brayne C, Welzel AT, Forster G, Shankar GM, et al. The presence of sodium dodecyl sulphate-stable Abeta dimers is strongly associated with Alzheimer-type dementia. Brain 2010; 133: 1328–41.

McDonald CR, Gharapetian L, McEvoy LK, Fennema-Notestine C, Hagler DJ Jr, Holland D, et al. Relationship between regional atrophy rates and cognitive decline in mild cognitive impairment. Neurobiol Aging 2012; 33: 242–53.

McGeer PL, McGeer EG. Anti-inflammatory drugs in the fight against Alzheimer's disease. Ann N Y Acad Sci 1996; 777: 213–20.

McGeer PL, McGeer EG. NSAIDs and Alzheimer disease: epidemiological, animal model and clinical studies. Neurobiol Aging 2007; 28: 639–47.

Mintun MA, Larossa GN, Sheline YI, Dence CS, Lee SY, Mach RH, et al. [11C]PIB in a nondemented population: potential antecedent marker of Alzheimer disease. Neurology 2006; 67: 446–52.

Morris JC, Storandt M, McKeel DW Jr, Rubin EH, Price JL, Grant EA, et al. Cerebral amyloid deposition and diffuse plaques in "normal" aging: Evidence for presymptomatic and very mild Alzheimer's disease. Neurology 1996; 46: 707–19.

Riley KP, Snowdon DA, Desrosiers MF, Markesbery WR. Early life linguistic ability, late life cognitive function, and neuropathology: findings from the Nun Study. Neurobiol Aging 2005; 26: 341–7.

Rowe CC, Ng S, Ackermann U, Gong SJ, Pike K, Savage G, et al. Imaging beta-amyloid burden in aging and dementia. Neurology 2007; 68: 1718–25.

Scheff SW, Price DA. Synaptic pathology in Alzheimer's disease: a review of ultrastructural studies. Neurobiol Aging 2003; 24: 1029–46.

Schneider JA, Aggarwal NT, Barnes L, Boyle P, Bennett DA. The neuropathology of older persons with and without dementia from community versus clinic cohorts. J Alzheimers Dis 2009; 18: 691–701.

Selkoe DJ. The molecular pathology of Alzheimer's disease. Neuron 1991; 6: 487–98.

Serrano-Pozo A, Mielke ML, Gomez-Isla T, Betensky RA, Growdon JH, Frosch MP, et al. Reactive glia not only associates with plaques but also parallels tangles in Alzheimer's disease. Am J Pathol 2011; 179: 1373–84.

Serrano-Pozo A, William CM, Ferrer I, Uro-Coste E, Delisle MB, Maurage CA, et al. Beneficial effect of human anti-amyloid-beta active immunization on neurite morphology and tau pathology. Brain 2010; 133: 1312–27.

Shankar GM, Li S, Mehta TH, Garcia-Munoz A, Shepardson NE, Smith I, et al. Amyloid-beta protein dimers isolated directly from Alzheimer's brains impair synaptic plasticity and memory. Nat Med 2008; 14: 837–42.

Spires TL, Meyer-Luehmann M, Stern EA, McLean PJ, Skoch J, Nguyen PT, et al. Dendritic spine abnormalities in amyloid precursor protein transgenic mice demonstrated by gene transfer and intravital multiphoton microscopy. J Neurosci 2005; 25: 7278–87.

Spires-Jones TL, Mielke ML, Rozkalne A, Meyer-Luehmann M, De Calignon A, Bacskai BJ, et al. Passive immunotherapy rapidly increases structural plasticity in a mouse model of Alzheimer disease. Neurobiol Dis 2009; 33: 213–20.

Tai HC, Serrano-Pozo A, Hashimoto T, Frosch MP, Spires-Jones TL, Hyman BT. The synaptic accumulation of hyperphosphorylated tau oligomers in Alzheimer disease is associated with dysfunction of the ubiquitin-proteasome system. Am J Pathol 2012; 181: 1426–35.

Tomic JL, Pensalfini A, Head E, Glabe CG. Soluble fibrillar oligomer levels are elevated in Alzheimer's disease brain and correlate with cognitive dysfunction. Neurobiol Dis 2009; 35: 352–8.

Van Exel E, Eikelenboom P, Comijs H, Frölich M, Smit JH, Stek ML, et al. Vascular factors and markers of inflammation in offspring with a parental history of late-onset Alzheimer disease. Arch Gen Psychiatry 2009; 66: 1263–70.

Watt AD, Perez KA, Rembach A, Sherrat NA, Hung LW, Johanssen T, et al. Oligomers, fact or artefact? SDS-PAGE induces dimerization of beta-amyloid in human brain samples. Acta Neuropathol 2013; 125: 549–64.

West MJ, Gundersen HJ. Unbiased stereological estimation of the number of neurons in the human hippocampus. J Comp Neurol 1990; 296: 1–22.

Wyss-Coray T. Inflammation in Alzheimer disease: driving force, bystander or beneficial response? Nat Med 2006; 12: 1005–15.